Turkish Journal of Engineering

https://dergipark.org.tr/en/pub/tuje

e-ISSN 2587-1366

Development of a sensitivity analysis tool for the trajectory of multistage launch vehicles

Ukte Aksen [*1], **Alim Rüstem Aslan** [2], **Ümit Deniz Göker** [3]

[1]*Istanbul Technical University, Department of Astronautical Engineering of Aeronautics and Astronautics, Türkiye, oneru@itu.edu.tr*
[1] *Aselsan Inc., Microelectronic Guidance and Electro-Optical Group, Ankara, Turkey, uaksen@aselsan.com.tr*
[2]*Istanbul Technical University, Department of Astronautical Engineering of Aeronautics and Astronautics, Türkiye, aslanr@itu.edu.tr*
[3]*Astronomical Institute of Czech Academy of Sciences, Department of Solar Physics, Fričova 298, 251 65, Ondřejov, Czech Republic, deniz.umit.goker@asu.cas.cz*

Cite this study: Aksen, U., Aslan, A. R., & Göker, Ü. D. (2024). Development of a sensitivity analysis tool for the trajectory of multistage launch vehicles. Turkish Journal of Engineering, 8 (2), 254-264

https://doi.org/10.31127/tuje.1379251

Keywords
Launch vehicles
Sensitivity analysis
Trajectory design

Research Article

Received: 21.10.2023
Revised: 12.12.2023
Accepted: 15.12.2023
Published: 09.04.2024

Abstract

The primary objective of this work is to create a highly accurate sensitivity analysis tool for multi-stage launch vehicle trajectories. This tool is designed to assess the impact of various parameters on the trajectory and performance of multi-stage launch vehicles. To achieve this, we have developed high-fidelity simulation software that considers all translational and angular movements by modelling the six-degrees-of-freedom (6DOF) equations of motion. The validation of this software is based on experimental data. An essential aspect of this work is the utilization of the developed sensitivity analysis tool to determine how different parameters affect the trajectory of multi-stage launch vehicles. Through the sensitivity analysis conducted using the developed tool, it is possible to identify which parameters are of critical importance during the design phase. We apply a generic mission profile for the Minotaur-I launcher to obtain parametric dependencies of the flight path. Through a comprehensive parametric study, we evaluate a range of critical parameters, including gross lift-off weight, a specific impulse of each stage, pitch-over manoeuvre initial time and angle, and ignition impulse of each stage. These parameters significantly influence the trajectory, performance, and reliability of the launch vehicle for mission design and success. The results of the sensitivity analysis underscore that even minor variations in these parameters can result in substantial deviations from the nominal insertion altitude. The acceptability of errors in specific impulse changes varies across stages, with maximum changes of 6.07%, and the fourth stage showing less sensitivity at 0.13%. However, it's important to note that variations in the parameters of the first stage tend to be challenging to rectify once they occur, with maximum changes in specific impulses reaching 75.57%. Another noteworthy discovery is that the acceptability of changes in pitch-over manoeuvre initiation times depends on the rate of change; they can be deemed either acceptable or unacceptable based on this factor, with changes ranging between 17.90% and 98.38%.

1. Introduction

Launch vehicles, also known as carrier rockets, serve the purpose of transporting one or more payloads from Earth's surface to space. They play a crucial role in various missions, including commercial and military satellite deployments, meteorological observation, and experimental research.

Throughout the history of the space race, a diverse range of launch vehicle systems has been developed. These systems are designed not only to access space but also to achieve their designated missions, contributing to the global prestige of the countries and organizations involved in space exploration.

The advancement of technology has amplified the significance of designing and determining trajectories for launch vehicles, particularly due to the intricate structures of modern launchers. Achieving a higher level of sophistication and success in specific missions necessitates precise modelling, simulation, and analysis of these launchers.

Various simulation tools for aerospace vehicles have been developed by numerous companies, agencies, and institutes. The objectives of these developers can vary. For instance, research centres at NASA have enhanced simulation tools like Core [1], JEOD [2], LaSRS++ [3], MAVERIC [4], POST2 [5], VMSRTE [6], and OTIS [7]. These tools offer distinctive features such as design and

flight performance analysis, modelling of object-oriented concepts and different vehicles in the same simulation platform, vertical motion simulation encompassing rotorcraft, trajectory generation, targeting, and optimization.

Additionally, simulation tools developed by Analysis, Simulation and Trajectory Optimization Software (ASTOS) Solutions GmbH and Artificial General Intelligence (AGI), namely ASTOS [8] and Systems Tool Kit (STK) [9], can conduct mission performance analysis, concept analysis, guidance, navigation, and control (GNC) design, modelling with high temporal and spatial accuracy, and employ cloud and server-based architecture while also facilitating vehicle orientation. In the existing literature, despite the availability of numerous simulation tools, it is important to note that many of them cannot perform sensitivity analysis.

The flight path and performance of a vehicle are influenced by a multitude of design and event parameters as well as modelling parametrization. Sensitivity analysis is a crucial step in understanding how vehicle performance is linked to these parameters. In essence, sensitivity analysis entails assessing how alterations in the input variables of a mathematical model or system impact the output variables under specific conditions. This analysis helps engineers and decision-makers understand the impact of uncertainties and variations in design parameters.

The performance sensitivity of a launch vehicle is multifaceted, encompassing various factors that influence its overall effectiveness. m_{pl} analysis delves into how alterations in payload mass (m_{pl}) can impact critical aspects like the maximum achievable orbit and payload capacity [10]. Similarly, propellant mass (m_p) fraction examination explores the launch vehicle's performance sensitivity to changes in the ratio of (m_p) to total mass (m_t). In terms of cost sensitivity, manufacturing costs, encompassing materials and production processes, are scrutinized for their impact on the overall launch vehicle cost. Operational costs, including launch site expenses and maintenance, are also analysed to understand their influence on the total cost of a launch [11]. Design parameter sensitivity involves studying the launch vehicle's structural response to variations in parameters like material strength, thickness, and geometry [12]. Environmental sensitivity considers the impact of weather conditions, such as wind and temperature variations, on launch vehicle performance and safety [13]. Additionally, the choice of launch site is assessed for its effect on performance, considering different atmospheric conditions and geographic considerations. System reliability sensitivity examines the overall launch system's reliability concerning variations in the reliability of individual components or subsystems. Finally, regulatory and policy sensitivity explores how changes in regulatory requirements, compliance standards, and government policies or international regulations can influence the design and operational aspects of the launch vehicle program [14].

Several sensitivity analysis methods, such as differential, factorial, and One-at-a-Time (OAT), are available. However, sensitivity analysis studies for multistage launch vehicles are notably scarce in the existing literature. While sensitivity analysis has been conducted in fields like aeroelasticity [15], structural loads [16], and cost modelling [17], only a single study exists that focuses on the sensitivity analysis of launch vehicle trajectories [18]. It's worth noting that this study employs a three-degrees-of-freedom (3DOF) flight mechanics model, which may not capture the true trajectory accurately. To achieve a precise trajectory estimation, accurate subsystem modelling, and sensitivity analysis are indispensable. Moreover, none of these studies include sensitivity analysis for trajectory or performance parameters.

To address this gap in the literature, a sensitivity analysis tool has been developed within the scope of this paper to derive flight, mission performance, and parametric dependencies of launch vehicles. The initial step involves modelling the Minotaur-I launch vehicle produced by the American Company, Orbital Sciences Corporation (OSC). This model serves to validate and verify the developed tool by comparing it with reference data from the launch vehicle's user guide.

Following the validation, a Six degrees-of-freedom (6DOF) flight mechanics model is implemented to ensure the tool's accuracy. Subsequently, the developed tool is employed to perform sensitivity analysis on the Minotaur-I launch vehicle. This analysis seeks to determine the impact of input parameters on the vehicle's trajectory and assess how accuracy varies with different input parameters.

The OAT method is selected for the sensitivity analysis, as it involves altering one input parameter at a time in each run, ensuring simplicity and clear attribution of observed changes in the mathematical model or system to the specific input parameter modifications.

In this study, a 6DOF comprehensive trajectory model is implemented and validated using Minotaur-I launch vehicle reference mission data. With the validated model, launch vehicle trajectories can be modelled without the need for high-cost or hard-to-access programs, allowing for the rapid generation of detailed results during the design phase. Furthermore, the model is user-friendly, innovative, and entirely under user control, making it adaptable to specific needs. In this context, a sensitivity analysis tool has been added to the model, enabling the examination of the sensitivity of different design and event variables and their effects on-orbit target parameters. This allows for an investigation into the impact of the user-desired parameters.

In the present study, the details of the modelling conducted are determined in Section 2 while the validation of the developed tool is given in Section 3. Section 4 involves sensitivity analysis, and the discussion and conclusion are given in Section 5.

2. Modelling

To create a sensitivity analysis tool, it is essential to establish a foundation comprising a generic flight dynamics model and environment models, including gravity and atmosphere models. Furthermore, a precise

implementation of subsystem models is required to accurately capture the characteristics of the launch vehicle. This necessitates the development of a 6DOF simulation model and the incorporation of environment models, which have been achieved through the utilization of MATLAB 2017b.

The tool also integrates propulsion, structural, and aerodynamic models for the launch vehicle. Specifically, the propulsion, structural, and aerodynamic models have been incorporated into the tool to enable comprehensive analysis.

In practice, the developed tool is employed to conduct sensitivity analysis for a specific launch vehicle. In this case, the Minotaur-I launch vehicle, produced by OSC, is selected as an exemplary launch vehicle to illustrate the tool's capabilities.

2.1. System dynamics

The trajectory model within simulation tools holds paramount importance, as it encompasses the entire set of equations of motion and transformation functions. Any inaccuracies or errors in the implementation of this model or the coupling of equations can result in irreparable consequences.

In the literature, various coordinate systems are available, and the Direction Cosine Matrix (DCM) is frequently employed for the conversion between these coordinate systems. In this study, the transformations considered are from Earth-Centered Earth-Fixed Frame (ECEF) to Earth-Centered Inertial Frame (ECI) and from ECEF to North-East-Down Frame (NED). The remaining frame rotation matrices are derived using either *q*-to-DCM or Euler angles-to-DCM functions, as documented in references [19–25].

In this study, an enhanced 6DOF modelling and simulation tool has been developed for aerospace vehicles. This tool encompasses both translational and angular motion aspects. Specifically, the study focuses on deriving the equations of rotational dynamics, which account for variations in time orientation. Additionally, it establishes the relationship between the derivative of the translational vector and angular velocity (ω).

The Moment vector (M) primarily results from the combined effects of aerodynamic forces and propulsion forces that do not act through the centre of mass. Furthermore, it incorporates the role of attitude control devices. Equation 1 demonstrates that the derivative of the angular momentum (h) of a rigid body, as measured in the inertial frame, is equivalent to the moment vector acting about the vehicle's centre of mass [26].

$$M = {}^{i}\dot{h}_{cm/i} \tag{1}$$

The notation, ${}^{i}\dot{h}_{cm/i}$ refers to the vector derivative of the ω of the body concerning the inertial frame, as observed from the inertial frame.

To derive the state equations for ω in body-fixed components, it is essential to introduce the Coriolis term to account for the rotation of the frame. This equation underscores the well-established fact that the angular momentum is equivalent to the product of the inertia matrix (J) and the ω. This understanding enables us to rearrange and substitute these terms into Equation 1 [26].

$${}^{b}\dot{\omega}_{b/i}^{bf} = \left(J^{bf}\right)^{-1}\left[\mathrm{M}^{bf} - \omega_{b/i}^{bf}\,\mathrm{x}\,J^{bf}\omega_{b/i}^{bf}\right] \tag{2}$$

In Equation 2, ${}^{b}\dot{\omega}_{b/i}^{bf}$ represents the components in the body coordinate system of the derivative taken in the body frame of the ω of the body concerning the inertial frame. Additionally, J^{bf} denotes the J for the rigid body. It's important to note that this matrix remains constant for an unchanging centre of mass (cm); however, it changes due to propellant consumption.

To derive the equation for translational motion, the second law of Newton is employed, aiming to calculate state parameters like the position and velocity vector (v) of a body. These calculations consider the impact of various forces such as aerodynamics, propulsion, gravitational attraction, and other disturbance forces.

However, it is also essential to account for centripetal and Coriolis accelerations, which arise due to the Earth's rotation and the movement of the frame. Following mathematical operations, the derivatives of the body's **v**, as observed in the body frame regarding the ECEF frame, have been determined, as expressed in Equation 3 [26].

$${}^{e}\dot{\mathbf{v}}_{cm/e} = \frac{1}{m}\mathbf{F} + \mathbf{G} - \omega_{e/i}x\left(\omega_{e/i}\,\mathrm{x}\,\mathbf{P}_{cm/O}\right) - 2\omega_{e/i}\mathrm{x}\mathbf{v}_{cm/e} \tag{3}$$

where F is the sum of forces vector, G is the gravitation vector of Earth, *O* is the cm of Earth, *m* is body mass and $\mathrm{P}_{cm/O}$ is body cm position with respect to *O*. In addition, the matrix form of state equations is given in Equation 4.

$$X = \left[q_{b/e}, \mathbf{P}_{b/e}^{e}, \mathbf{v}_{b/e}^{e}, \omega_{b/i}^{e}\right]^{T} \tag{4}$$

where $q_{b/e}$ is quaternions of the body concerning ECEF, $\mathrm{P}_{b/e}^{e}$ is the components in the ECEF frame of the P of the body concerning ECEF, $\mathrm{v}_{b/e}^{e}$ is the components in the ECEF frame of the v of the body about ECEF and, $\omega_{b/i}^{e}$ is the components in ECEF frame of the **h** of the body concerning to ECI. The fourth-order Runge-Kutta Integration Method is used to solve differential equations [27].

2.2. Environment models

Environmental changes significantly impact the performance and stability of aerospace vehicles. The influence of these changes depends on various factors specific to the type of vehicle. In the case of launch vehicles, two paramount factors are the Earth's atmosphere and its gravity field. As a result, the tool incorporates models for both gravity and atmosphere to address these key considerations.

To achieve a trajectory that accurately replicates the behaviour of aerospace vehicles as they move across the Earth's surface, it is imperative to possess a precise model for the Earth's shape. *The World Geodetic System 1984* Model plays a crucial role in providing highly accurate information about the ellipsoidal shape of the Earth. Over the years, this model has seen refinements,

with the most recent update in 2013 boasting an impressive accuracy of 1 cm [28].

The parameters that define the Earth's oblate spheroid shape, along with their most widely recognized abbreviations, are detailed in Table 1 [29]. It's worth noting that the gravitational constant in this context is geocentric and accounts for the mass of Earth's atmosphere.

Table 1. The WGS-84 parameters [29].

Parameter	Abbreviation	Value	Unit
Semi-major axis	a	6378137	m
Semi-minor axis	b	6356752	m
Angular velocity	ω	7.292115 x 10^{-5}	rad/s
Flattening	f	1/298.2572235	-
Gravitational constant	GM	3986.5	km^3/s^2
Eccentricity	e	0.081819190	-

In recent years, significant advancement has been made in the form of the EGM2008 Gravity Model, which is a global high-degree potential model [30]. This model has proven to be crucial for accurately calculating the trajectory of aerospace vehicles.

To facilitate the utilization of this model, the parameters listed in Table 1 are employed. By simplifying the gravitational potential function, a function for gravitational acceleration concerning the ECEF frame is derived. This function is then integrated into the tool, and it is represented in Equation 5 [31].

$$G_{J_2}^{ECEF} = -\frac{3}{2}J_2\left(\frac{\mu}{r^2}\right)\left(\frac{a}{r}\right)^2\begin{bmatrix}\left(1-5\left(\frac{z}{r}\right)^2\right)\frac{x}{r}\\ \left(1-5\left(\frac{z}{r}\right)^2\right)\frac{y}{r}\\ \left(1-5\left(\frac{z}{r}\right)^2\right)\frac{z}{r}\end{bmatrix} \quad (5)$$

where x, y, and z are ECEF position, μ is Earth's gravitational constant, r is the distance from the centre of mass of Earth, a is the semi-major axis of WGS84 ellipsoid and J_2 is the zonal harmonic coefficient.

Two categories of atmosphere models exist: reference and standard atmosphere models. While standard atmosphere models primarily consider the vertical distribution of atmospheric properties solely about h_{alt}, reference models encompass a broader range of factors, including seasonal, geomagnetic, solar, and latitude effects. Consequently, reference models tend to offer higher accuracy than standard models.

In the context of this study, the US1976 Standard Atmosphere Model has been adopted. The additional influences covered by reference models are not deemed critical to the research objectives. In this model, h_{alt} is the sole input parameter, while absolute temperature in Kelvins (T), Pressure (P), speed of sound (u), and atmospheric density (ρ) are the resulting outputs. These outputs are used to calculate parameters such as Mach number (M) and dynamic pressure (P_{dyn}).

The model can provide data up to a h_{alt}=84 km [32]. For h_{alt} beyond 84 km, the model relies on a look-up table. To extend its applicability, new functions have been created through a curve-fitting method using the data from this table. As a result, the implemented model remains valid up to a h_{alt}=1000 km [32].

For speed of sound (Equation 6) [33],

$$u = \sqrt{\frac{\gamma_{ad}RT}{M}} \quad (6)$$

where adiabatic index $(\gamma_{ad}) = 1.4$, universal gas constant $(R) = 8314.15$ Nm/kmolK, molecular mass $(M) = 28.95$ kg/kmol.

For Mach number (Equation 7) [33],

$$\mathrm{M} = \frac{V}{u} \quad (7)$$

For M which is used in the calculation of ρ is obtained by curve fitting. The density equation is given in the Equation 8 [34].

$$\rho = \frac{P_{atm}M}{RT} \quad (8)$$

The dynamic pressure equation is given in Equation 9 [34].

$$P_{dyn} = \frac{1}{2}\rho V^2 \quad (9)$$

here, V is the velocity magnitude of the vehicle.

2.3. Propulsion model

The Minotaur-I launch vehicle, which is the subject of this study, comprises four stages powered by solid propellant. The vehicle's properties are detailed in Table 2 [35]. Furthermore, it's noteworthy that this launch vehicle has undergone a total of eleven launches, and each mission has achieved success.

The choice to focus on a multistage launch vehicle with solid motors is deliberate. This selection is driven by the need to implement a sloshing model, which is particularly relevant for liquid and hybrid rocket motors and is expected to enhance the overall accuracy of the study.

Changes in h_{alt} have a direct impact on the total thrust generated by the launch vehicle, mainly because atmospheric pressure (P_{atm}) varies in h_{alt}. To ensure precision in the results, a P correction is applied by utilizing the vacuum thrust (T_{vac}) data for each stage, which is available from the vehicle's user guide [36].

The actual thrust magnitude (T_{thrust}) concerning h_{alt} is expressed in Equation 10 [33]. This equation is instrumental in determining how thrust varies with changing h_{alt}.

$$T_{thrust} = T_{vac} - p_3A_2 \quad (10)$$

Furthermore, the amount of propellant necessary for mission manoeuvres is easily calculated using the Tsiolkovsky rocket equation. This calculation is succinctly presented in Equation 11 [33].

In Equation 11, m_p is the propellant mass consumed to produce the needed v, and ΔV is the v increase of the vehicle and mi is the initial vehicle mass.

$$m_p = m_i \left[1 - \exp\left(-\frac{\Delta V}{g_0 I_{sp}}\right)\right] \quad (11)$$

Table 2. Minotaur I Launch vehicle characteristics [35].

	Stage 1 MM 55A1	Stage 2 MM SR19	Stage 3 Orion 50XL	Stage 4 Orion 38
Dimensions				
Length (m)	7.49	4.12	3.07	1.34
Diameter (m)	1.67	1.33	1.28	0.97
Mass (each)				
Propellant mass (kg)	20,785	6,237	3,645	770,2
Gross Mass (kg)	23,077	7,032	4,036	872,3
Structure				
Type			Monocoque	Monocoque
Case Material	D6AC Steel	6Al-4V Titanium	Graphite Epoxy	Graphite Epoxy
Propulsion				
Propellant	Solid TP-H1011	Solid ANB-3066	HTPB	HTPB
Thrust (kN) (Vacuum)	792	267.7	194.4	36.9
Isp (sec) (Vacuum)	262	288	289	287
Control-Pitch, Yaw	TVC ±8o	LITVC	EMA ±3 o	EMA ±3 o
Roll	TVC ±8 o	Warm gas RCS	Nitrogen cold gas RCS	Nitrogen cold gas RCS
Events				
Nominal Burn Time (sec)	61.3	66	71	66.8
Stage Shutdown	Burn to depletion	Burn to depletion	Burn to depletion	B-urn to depletion
Stage Separation			Spring ejection	Spring ejection

2.4. Structural model

The vehicle's structure serves as both a mechanical interface connecting the launch vehicle stages and the primary structural support for all subsystems. As a result, it's crucial to determine the most optimal structural configuration for the vehicle to meet mission requirements.

The modelling of the vehicle is carried out using CATIA V15R19 product design software. Given that the materials for each stage are known, the volumes of the structural components can be determined. Additionally, propellant volumes and heights are calculated based on the propellant density and the volume of the structural parts. This comprehensive approach allows for precise design and configuration of the vehicle's structure to meet the specific mission requirements.

2.5. Aerodynamics model

During the flight of launch vehicles, the three components of aerodynamic forces and moments acting on the vehicle are influenced by a combination of factors, including the vehicle's configuration, environmental properties, and its attitude relative to the free stream velocity [37]. Specifically, this study considers three aerodynamic forces: drag, lift, and side force, as well as three aerodynamic moments: rolling, pitching, and yawing moment, which all act on the launch vehicles.

The aerodynamic coefficients, which play a significant role in these forces and moments, depend on various parameters. However, for this study, they are modelled to be dependent on three primary parameters: α, β, and M. The angle of attack (α) and sideslip angle (β) are considered within the range of -20 to 20 degrees, while the M spans from 0 to 50. These parameters are central to the modelling of aerodynamic behaviour in the study.

In the early stages of aircraft design, engineers use the DATCOM semi-empirical aerodynamic prediction tool to obtain crucial aerodynamic characteristics. This tool combines theoretical methods with empirical data from wind tunnel tests and flight experiments, providing a relatively quick and accurate estimation of aerodynamic properties [38]. Consequently, parameters like mesh structure and flow domain, common in Computational Fluid Dynamics (CFD) solutions, cannot be addressed. While more detailed aerodynamic coefficient predictions can be achieved with CFD in later design stages, this study focused on the early design phases. The launch vehicle, experiencing intense aerodynamic effects in a short time, prompted the use of the DATCOM tool for a swift and efficient solution.

For this study, the aerodynamic coefficients are derived using DATCOM Revision 2011, employing the example configuration of the Minotaur-I launch vehicle, as depicted in Figure 1. DATCOM is a widely utilized semi-empirical aerodynamic prediction tool, capable of projecting aerodynamic forces, moment coefficients, and stability derivatives as functions of the α and M [38].

The process involves inputting the vehicle's configuration into DATCOM, and then the code is executed multiple times to obtain coefficients for varying β values. Furthermore, the aerodynamic computations for the launch vehicle encompass the incorporation of stability derivatives of these coefficients.

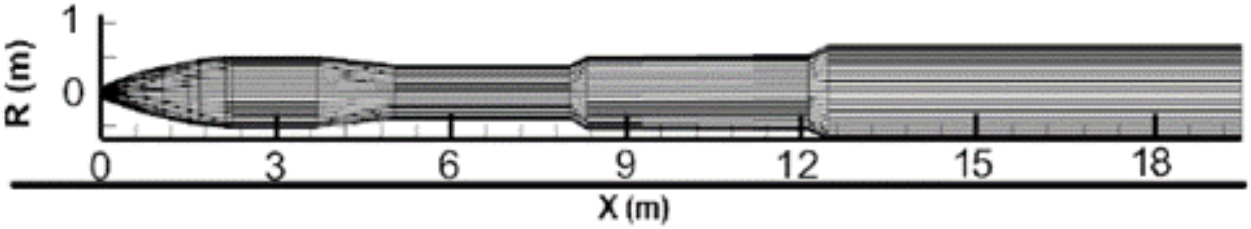

Figure 1. Minotaur-I vehicle configuration.

3. Reference mission and verification

The Minotaur-I launch vehicle is designed to transport payloads into both Low Earth Orbit (LEO) and Sun-Synchronous Orbit (SSO). To facilitate the sensitivity analysis, it's essential to validate the developed tool. For this purpose, a specific mission is selected from the launch vehicle's user guide [36]. In this mission, the vehicle is launched from Vandenberg Air Force Base Launch Platform, situated at a longitude of 120° 37' 56.57" W, a latitude of 34° 34' 34.86" N, and a h_{alt}=117 meters above sea level. The payload for this mission weights 302 kg, and the objective is to place it in a circular SSO with an inclination (i)=98°.3°, at a h_{alt}=741.3 km, and a **v**=7482.2 m/s [36]. A SSO is a nearly polar orbit around a planet. In this orbit, a satellite passes over any given point on the planet's surface at the same local mean solar time. On the other hand, the LEO region refers to the area of space below a h_{alt}=2,000 km, which is approximately one-third of Earth's radius. It is selected because SSO is a special type of LEO, and the experimental data used in the study are accessible for open access. The proposed study can be applied to all LEO missions that do not require agile manoeuvres of the launch vehicle for placing the satellite into orbit.

Simulation outputs for the reference mission were obtained from the developed tool. To validate the tool, the efficiency of using the v and h_{alt} values of nine reference points extracted from the user's guide's reference case, provided by the manufacturer, as verification data, is evident when comparing the results obtained. The comparison of h_{alt} reference data and the results obtained from the developed tool is shown in Figure 2, while the v comparison is illustrated in Figure 3. Different colours and line styles are used for each stage of the launch vehicle in the figures, while "x" markers are employed for reference data.

Additionally, to accurately position the payload into its target orbit, it's crucial to achieve a γ of approximately zero degrees. The flight path angle (γ) is calculated as the difference between pitch angle (θ) and α, as expressed in Equation 12.

$$\gamma = \theta - \alpha \tag{12}$$

The result of the tool for γ is given in Figure 4. When examining the figures, it is observed that the marked reference data aligns with the results of the developed tool for h_{alt} and v. At the final stage, particularly when reaching stage 4, simulation results should meet the target parameters. The developed tool has calculated the final values for γ to be approximately 0.015°, h_{alt} to be 741.5 km, and v to be 7496 m/s. These values closely align with those specified in the vehicle's user guide.

Figure 2 illustrates that as the simulation progresses, altitude increases, reaching the targeted orbit altitude, and drop altitudes for each stage are observed. In Figure 3, it is evident that fuel consumption increases the velocity for each stage, followed by a gradual decrease after the end of combustion until reaching the targeted speed. In Figure 4, the launch vehicle initially rises vertically upon liftoff, undergoes a gravity turn maneuver, and approaches a flight path angle near zero when reaching the targeted orbit altitude. Points marked with x for γ, h_{alt}, and **v** parameters have error rates calculated concerning reference values, revealing a maximum difference of 1.7% between simulation results and reference points for all three parameters. Due to the significantly low maximum difference, it is evaluated that the developed tool exhibits high accuracy and can be utilized in precision analysis. Since there is no reference value for the flight path angle, its proximity to zero upon reaching the targeted orbit is crucial. Table 3 presents a comparison of Minotaur-I launch vehicle simulation results and experimental results, including error values for altitude and velocity.

The injection accuracy, as expected [36], is smaller than the resolution for accuracy, with a margin of ± 55.6 km for mean h_{alt} and ±0°.2 for i. These slight deviations can be attributed to numerous unknown parameters involved in the modelling process, including environmental perturbations and aerodynamic inconsistencies.

For instance, variations may arise from differences in aerodynamic coefficient inputs, such as the α and β. Other crucial factors in the aerodynamic model include the choice of atmosphere model and M.

It is important to emphasize that the accuracy of the results depends on faithfully implementing the vehicle's configuration and properties. Therefore, this tool proves valuable for sensitivity analysis due to its precision, reliability, and efficiency. Furthermore, it offers the advantage of easier user-friendly improvements compared to commercial software.

Table 3. Comparison of Minotaur-I launch vehicle simulation results and experimental results.

Parameter	Simulation result	Experimental results	% Error
Altitude (km)	741.5	741.3	0.027
Velocity (m/s)	7496	7482.2	0.184

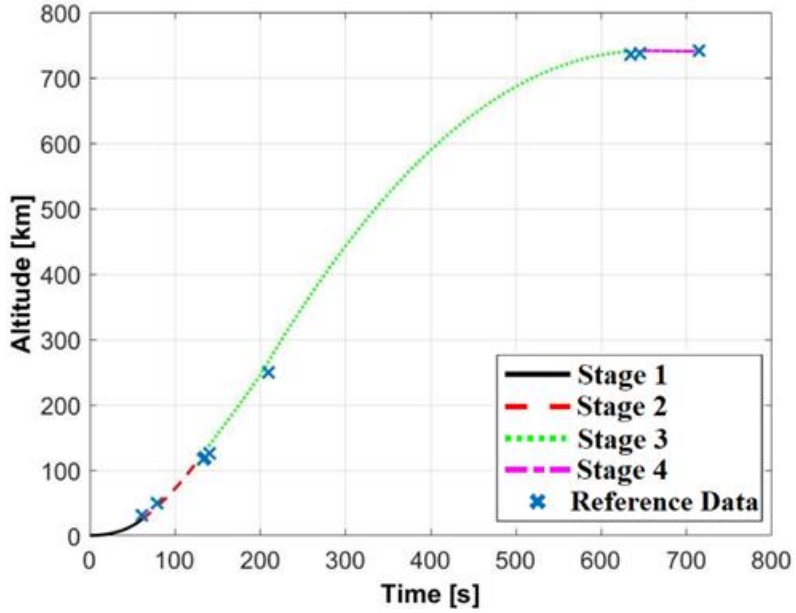

Figure 2. Altitude comparison of Minotaur-I launch vehicle for reference case.

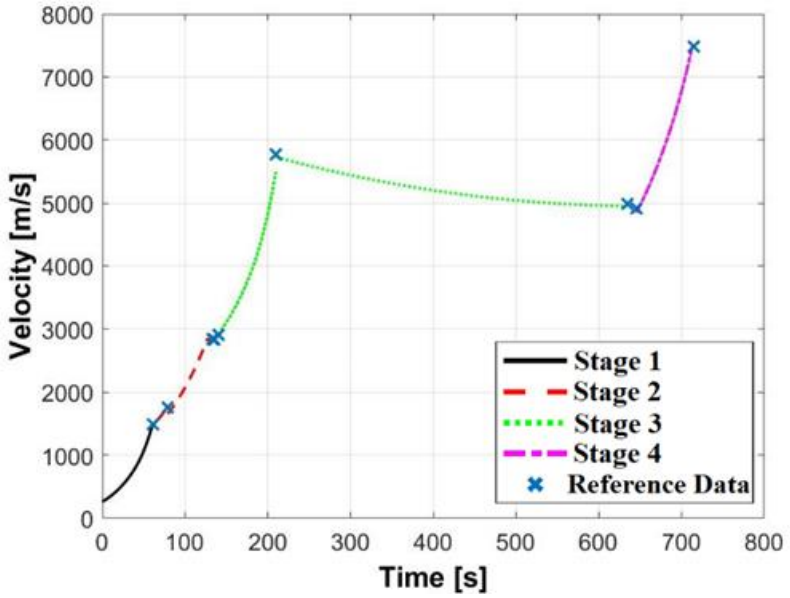

Figure 3. Velocity comparison of Minotaur-I launch vehicle for reference case.

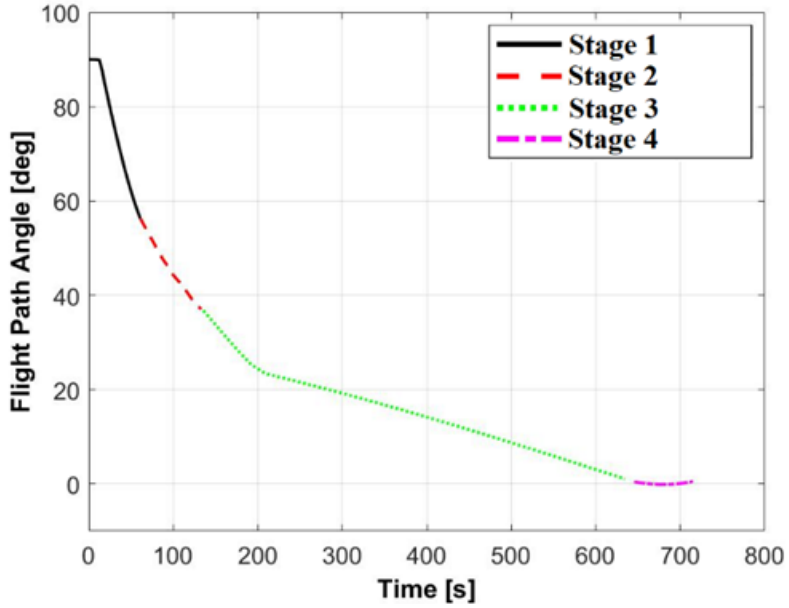

Figure 4. Minotaur-I flight path angle results with respect to time for reference case.

4. Sensitivity analysis

A sensitivity analysis was conducted for the Minotaur-I launch vehicle using the vehicle's implemented subsystem models. The vehicle's trajectory and performance are influenced by numerous design and event parameters. To assess the impact on the mission, the analysis considered factors such as the gross lift-off weight, I_{sp} of each stage, pitch-over manoeuvre starts time, ignition time of upper stages, and pitch-over manoeuvre angle.

Although changes in these parameters affect the entire set of state variables, the results are presented in h_{alt} relative to the variation parameter graph. h_{alt} is the preferred parameter for illustrating such variations and is most comprehensible to readers. The parameters and their variations used in the sensitivity analysis are summarized in Table 4.

Table 4. The summary of sensitivity parameters.

Symbol	Parameters	Variation
x_1	GLOW	(-100) - (50) kg
x_2	I_{sp_1}	(-4) % - (4) %
x_3	I_{sp_2}	(-4) % - (4) %
x_4	I_{sp_3}	(-4) % - (4) %
x_5	I_{sp_4}	(-4) % - (4) %
x_6	pitch-over final time	(-10) - (10) s
x_7	pitch-over start time	(-10) - (10) s
x_8	stage 2 ignition	(-10) - (10) s
x_9	stage 3 ignition	(-10) - (10) s
x_{10}	stage 4 ignition	(-10) - (10) s
x_{11}	TVC angle	(-1)-(1) deg

The Gross Lift-Off Weight (GLOW) is a crucial measure encompassing the total weight of the launch vehicle at the lift-off stage, including the main rocket structure, propellant, payload, and boosters. This parameter holds significant importance in trajectory planning and launcher design. The Minotaur-I launch vehicle, for example, weights approximately 32 tonnes [36].

Another key parameter under scrutiny is the specific impulse at vacuum, denoted as I_{sp}. It is examined with variations of ±8% from its actual value for each stage individually. Alongside design variables, the control parameters for various events play a critical role in determining the vehicle's trajectory.

The launch vehicle initiates its ascent vertically from the Earth's surface and must perform a pitch-over manoeuvre to achieve the target orbit with the required γ. Therefore, precision in manoeuvre timing is vital for mission success. The second control parameter involves the ignition time of the upper stages. These stages commence their burn once the lower stages separate and reach the necessary h_{alt} as dictated by the mission. Failure to ignite at the precise moment could lead to the payload missing the target orbit.

Furthermore, the Thrust Vector Control (TVC) angle is employed following the initial vertical ascent to initiate the gravity turn manoeuvre, which is essential for achieving the desired γ. Failing to maintain the correct angle could result in the payload not reaching the intended orbit. The results of these sensitivity parameters are depicted in Figure 5.

The sensitivity analysis encompasses various design parameters, including the GLOW and the I_{sp} of each stage, as well as event-related parameters like ignition times, pitch-over manoeuvre initiation times, and manoeuvre angles.

It's seen that any deviations in mass can lead to mission failure, but a control mechanism can be employed to achieve the target parameter. The I_{sp} value of the first stage holds greater significance due to its substantial influence on the trajectory. As we progress from stage 1 to stage 4, the number of values within the accuracy limits increases because the vehicle's mass generally decreases, and the final stage is responsible for orbit injection.

The timing of the initiation has a vital impact on the launch vehicle's flight path, particularly when the vehicle maintains motion with a large γ, resulting in a h_{alt} higher than nominal. For example, a deviation of about 10 seconds, whether early or delayed, in the manoeuvre initiation, is intolerable due to accuracy constraints. However, a 2-second deviation remains within acceptable limits.

The ignition times of the stages significantly affect the trajectory, with the second stage ignition time having the most pronounced impact. The dependency decreases as we move from stage 1 to stage 4. To illustrate, a 5-second delay in the ignition of the second stage is unacceptable, while it may be allowable for the fourth stage.

In this mission simulation, the nominal value for the manoeuvre angle is 4.75 degrees. Results indicate that even a 0.5-degree deviation from the actual value can lead to significant changes in apogee h_{alt}. The most substantial deviation is observed in the first stage and the pitch-over manoeuvre angle, as per the sensitivity analysis results. Small variations in these parameters can result in critical consequences, such as accidents resulting in fatalities or mission failure. Consequently, achieving a higher level of modelling accuracy is imperative for mission success.

The errors in trajectory can stem from various sources, including motor performance, uncertainties in

the guidance algorithm, and navigation issues. In many instances, deviations in injection h_{alt} can be accommodated within the Minotaur-I launch vehicle's specified accuracy limits. However, most cases analysed in the sensitivity study exceed these limits and cannot be dismissed as negligible.

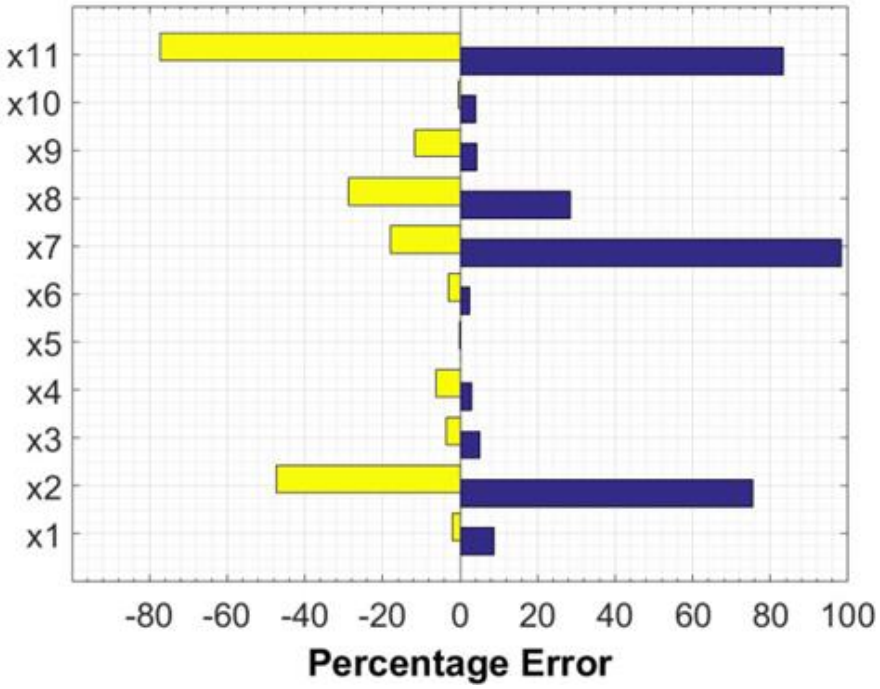

Figure 5. The results of sensitivity analysis.

Conversely, certain scenarios, such as those involving the fourth stage, could have noticeable implications. This is particularly relevant because the final stage is typically employed to achieve specific payload orbit parameters rather than gaining h_{alt}.

Addressing these potential errors necessitates a meticulous approach, involving careful design, pre-flight analysis, Monte-Carlo simulations, and control systems aligned with the predetermined trajectory to mitigate and manage issues effectively.

5. Discussion and Conclusion

During this study, a sensitivity analysis tool was developed, which includes a 6DOF trajectory model for aerospace vehicles. This tool can predict the trajectories of both currently operational and under-development launch vehicles designed for LEO with a high degree of accuracy within a short time frame.

ASTOS emerges as a prominent aerospace modelling tool, excelling in orbit and trajectory analysis, which proves indispensable for meticulous space mission planning and optimization. Its advanced spacecraft dynamics modelling capabilities, accurately representing propulsion systems and mission profiles, position ASTOS as the preferred choice for intricate space missions. Notables are ASTOS optimization features, allowing users to fine-tune trajectories based on diverse constraints. However, challenges include a steeper learning curve and a specialization in space mission analysis, potentially limiting its adaptability for broader aerospace applications like aircraft flight dynamics [39]. In contrast, the STK distinguishes itself with versatility, supporting multi-domain simulation across space missions, aircraft, unmanned aerial vehicles (UAVs), missiles, and ground systems. Yet, it may not match the detailed spacecraft dynamics modelling of specialized tools like ASTOS, and its optimization capabilities may lack the specificity required for intricate trajectory planning [40]. On the other hand, NASA and ASTOS programs are high-cost and difficult or inaccessible programs. In the developed tool, there is modelling and simulation capability for satellite launch vehicles that require manoeuvres such as gravity turn and capability of TVC, compared to other programs. In addition, its advantages compared to other programs include the ability to provide the user with the option to choose a method or integrate their algorithm according to the user's needs for optimization or integration solutions. Furthermore, it enables sensitivity analysis by incorporating comprehensive models as needed by the user.

The developed tool not only provides rapid solutions but also opens possibilities for using it during the development phase of launch vehicles to optimize their trajectories according to specific requirements. To validate the tool, it was compared with reference mission data obtained from the user's guide for the Minotaur-I launch vehicle.

This analysis encompasses a wide range of design and event parameters, utilizing the properties and subsystems of the Minotaur-I launch vehicle. The translational and rotational equations of motion are based on Newtonian principles, incorporating Earth's rotation and ellipsoidal shape. Quaternion updates are employed for attitude orientation during rotational motion, and a fourth-order Runge-Kutta integration method is used for system dynamics calculations. To simulate the environment, gravity, and atmospheric models are utilized. The EGM2008 gravity model is

chosen for its precision, and the US Standard Atmosphere Model 1976, considering h_{alt}, is used due to its simplicity and lack of seasonal effects.

For the reference mission verification, the Minotaur-I thrust profile was determined, accounting for factors such as P corrections and structural property changes, including the J, m, and centre of gravity. Structural properties were obtained using CATIA V15R19 product design software, while aerodynamic coefficients were determined using DATCOM Revision 2011 for all stages. The analysis does not assume any simplifications and considers all three axes of aerodynamic forces and moments acting on the vehicle. When the tool results and reference data are compared, it has been observed that the tool results align with the reference Minotaur-I mission data.

After verifying the developed tool by comparing it to reference mission data, sensitivity analysis has been carried out using the verified tool. The results of the sensitivity analysis highlight that even minor variations in these parameters can lead to significant differences in insertion h_{alt} compared to the nominal value. While GLOW changes can be tolerated for slight variations, changes in pitch-over manoeuvre angles are less forgiving. Like GLOW, the acceptability of errors in I_{sp} changes for the second and third stages varies, with errors being more negligible for the fourth stage. However, variations in the first stage parameters are generally irrecoverable.

Another significant finding is that changes in pitch-over manoeuvre initiation times can be either acceptable or unacceptable, depending on the rate of change. These errors may result from a range of factors, including motor performance, uncertainties in guidance algorithms, and navigation problems, and their tolerance is determined based on vehicle accuracy limits and control system properties.

In summary, the study has developed a sensitivity analysis tool for aerospace vehicles, demonstrating that accurate modelling of subsystems can yield real trajectories and provide insights into vehicle performance and parameter dependencies. Precise modelling is of utmost importance for mission success. During the design phase, the validated model streamlines the modelling of launch vehicle trajectories without the requirement for high-cost or hard-to-access programs, facilitating the swift generation of detailed results. Furthermore, the model, known for its user-friendly interface, innovation, and complete user control, ensures adaptability to specific needs. Within this framework, the model integrates a sensitivity analysis tool, allowing for the examination of various design and event variables and their effects on-orbit target parameters. This arrangement facilitates an investigation into the impact of user-desired parameters.

6. Future works

The possible further studies are listed as:

- Expanding the simulation and analysis beyond solid propellants to include a sloshing model for liquid propellants, which can significantly impact the system dynamics of launch vehicles.
- Integration of a disturbance model into the environment model to account for atmospheric conditions.
- Implementation of Guidance, Navigation, and Control (GNC) algorithms to enhance the fidelity of simulations.

Acknowledgement

Grant number MDK-2019-41839 supported this research, with funding provided by ITU Coordinatorship of Scientific Research Projects.

Author contributions

Ukte Aksen: Conceptualization, Methodology, Visualization, Validation, Writing. **Alim Rüstem Aslan:** Conceptualization, Methodology, Writing-Reviewing and Editing. **Ümit Deniz Göker:** Visualization, Investigation, Writing-Reviewing and Editing.

Conflicts of interest

The authors declare no conflicts of interest.

References

1. Castro, M. P. (2015). AFRC Core Simulation Overview (No. AFRC-E-DAA-TN23131).
2. Stewart, S. M., Ward, L., & Strand, S. Distributed GN&C Flight Software Simulation for Spacecraft Cluster Flight. In Proceedings of the 37th Annual AAS Guidance and Control Conference, AAS, 14-32.
3. Leslie, R., Geyer, D., Cunningham, K., Glaab, P., Kenney, P., & Madden, M. (1998). LaSRS++-An object-oriented framework for real-time simulation of aircraft. In AIAA Modeling and Simulation Technologies Conference and Exhibit, 382-388. https://doi.org/10.2514/6.1998-4529
4. Phys.org. (2004). Marshall Center names flight simulator 2004 'Software of the Year'. https://phys.org/news/2004-07-marshall-center-flight-simulator-software.html
5. Zwack, M. R., Dees, P. D., Thomas, H. D., Polsgrove, T. P., & Holt, J. B. (2017). Program to Optimize Simulated Trajectories II (POST2) Surrogate Models for Mars Ascent Vehicle (MAV) Performance Assessment (No. NASA/TM-2017-219842).
6. Anton, P. S., Raman, R., Osburg, J., & Kallimani, J. G. (2009). An Update of the Nation's Long-Term Strategic Needs for NASA's Aeronautics Test Facilities. The RAND Corporation, Santa Monica, CA.
7. NASA. (2008). OTIS 3.2 Software Released. https://ntrs.nasa.gov/api/citations/20050215610/downloads/20050215610.pdf
8. Cremaschi, F., Weikert, S., Schäff, S., & Wiegand, A. (2018). ASTOS, a reconfigurable software for design of mega constellations, operation of Flying Laptop and end-of-life disposal. In 2018 SpaceOps Conference (p. 2496).
9. AGI website (2018). http://www.agi.com/home.
10. Kirkpatrick, D. (1999). Space mission analysis and design, 8. Torrance: Microcosm.

11. Aguirre, M. A. (2012). Introduction to space systems: design and synthesis, 27. Springer Science & Business Media.
12. Sarafin, T. P., & Larson, W. J. (1995). Spacecraft structures and mechanisms: from concept to launch. Springer Dordrecht
13. Cornelisse, J. W., Schöyer, H. F. R., & Wakker, K. F. (1979). Rocket Propulsion and Spaceflight Dynamics. Aerospace Engineering Series. Pitman.
14. Diederiks-Verschoor, I. H. (2008). An introduction to space law. Kluwer Law International.
15. Mastroddi, F., Stella, F., Polli, G. M., & Giangi, M. (2008). Sensitivity analysis for the dynamic aeroelasticity of a launch vehicle. Journal of Spacecraft and Rockets, 45(5), 999-1009. https://doi.org/10.2514/1.30725
16. McGhee, D. S., Peck, J. A., & McDonald, E. J. (2012). Probabilistic Sensitivity Analysis for Launch Vehicles with Varying Payloads and Adapters for Structural Dynamics and Loads. In 14th AIAA Non-Deterministic Approaches Conference, M11-0845.
17. Yang, S. S. (2020). Sensitivity Analysis of Major Cost Parameters on the Launch Cost of Reusable Vehicles. Journal of the Korean Society of Propulsion Engineers, 24(2), 35-42. https://doi.org/10.6108/KSPE.2020.24.2.035
18. Jodei, J., Ebrahimi, M., & Roshanian, J. (2009). Multidisciplinary design optimization of a small solid propellant launch vehicle using system sensitivity analysis. Structural and Multidisciplinary Optimization, 38, 93-100. https://doi.org/10.1007/s00158-008-0260-5
19. Kresse, W., & Danko, D. M. (Eds.). (2012). Springer handbook of geographic information, 118-120. Berlin, Springer.
20. Chang, K. T. (2008). Introduction to geographic information systems (Vol. 4). Boston: McGraw-Hill.
21. Cai, G., Chen, B. M., & Lee, T. H. (2011). Unmanned rotorcraft systems. Springer Science & Business Media.
22. Hotine, M. (1991). Geodetic coordinate systems. In Differential Geodesy, 65-89. Berlin, Heidelberg: Springer Berlin Heidelberg.
23. Seemkooei, A. A. (2002). Comparison of different algorithms to transform geocentric to geodetic coordinates. Survey Review, 36(286), 627-633.
24. Janota, A., Šimák, V., Nemec, D., & Hrbček, J. (2015). Improving the precision and speed of Euler angles computation from low-cost rotation sensor data. Sensors, 15(3), 7016-7039. https://doi.org/10.3390/s150307016
25. Tewari, A. (2011). Advanced control of aircraft, spacecraft and rockets. John Wiley & Sons.
26. Stevens, B. L., Lewis, F. L., & Johnson, E. N. (2015). Aircraft control and simulation: dynamics, controls design, and autonomous systems. John Wiley & Sons.
27. Christodoulou, N. S. (2009). An algorithm using Runge-Kutta methods of orders 4 and 5 for systems of ODEs. International Journal of Numerical Methods and Applications, 2(1), 47-57.
28. Malys, S., Wong, R., & True, S. A. (2016). The WGS 84 terrestrial reference frame in 2016. In Eleventh Meeting of the International Committee on GNSS, ICG-11, 6-11.
29. International Civil Aviation Organization (2002). World Geodetic System, 1984 (WGS-84) Manual.
30. Amin, M. M., El-Fatairy, S. M., & Hassouna, R. M. (2002). A Better Match of the EGM96 Harmonic Model for the Egyptian Territory Using Collocation. Port-Said Engineering Research Journal PSERJ, 6(2), 1-16.
31. Markley, F. L., & Crassidis, J. L. (2014). Fundamentals of Spacecraft Attitude Determination and Control. Space Technology Library. Springer New York
32. Atmosphere, U. S. (1976). US standard atmosphere. National Oceanic and Atmospheric Administration.
33. Sutton, G. P., & Biblarz, O. (2016). Rocket propulsion elements. John Wiley & Sons.
34. Tewari, A. (2007). Atmospheric and space flight dynamics. Birkhũser Boston.
35. Buckley, M. S., Weis, C. S., Marina, L. L., Morris, L. C., & Schoneman, S. (1998). The Orbital/Suborbital Program (OSP)" Minotaur" Space Launch Vehicle: Using Surplus ICBM Motors to Achieve Low Cost Space Lift for Small Satellites.
36. Minotaur (2020). Minotaur I User's Guide. Northrop Group.
37. Suresh, B. N., & Sivan, K. (2015). Integrated design for space transportation system, 142-143. New Delhi: Springer India.
38. Sooy, T. J., & Schmidt, R. Z. (2005). Aerodynamic predictions, comparisons, and validations using missile datcom (97) and aeroprediction 98 (ap98). Journal of Spacecraft and Rockets, 42(2), 257-265. https://doi.org/10.2514/1.7814
39. Morante, D., Sanjurjo Rivo, M., & Soler, M. (2021). A survey on low-thrust trajectory optimization approaches. Aerospace, 8(3), 88. https://doi.org/10.3390/aerospace8030088
40. Borg, L. (2023). Concept investigation into metal plasma source for high powered space applications.